Cellular/Molecular

Nuclear Factor E2-Related Factor 2-Dependent Antioxidant Response Element Activation by *tert*-Butylhydroquinone and Sulforaphane Occurring Preferentially in Astrocytes Conditions Neurons against Oxidative Insult

Andrew D. Kraft,[1] Delinda A. Johnson,[1] and Jeffrey A. Johnson[1,2,3]

[1]School of Pharmacy, [2]Waisman Center, and [3]Molecular and Environmental Toxicology Center, University of Wisconsin, Madison, Wisconsin 53705

Binding of the transcription factor nuclear factor E2-related factor 2 (Nrf2) to the antioxidant response element (ARE) in neural cells results in the induction of a battery of genes that can coordinate a protective response against a variety of oxidative stressors. In this study, *tert*-butylhydroquinone (tBHQ) and sulforaphane were used as activators of this pathway. Consistent with previous studies, treatment of primary cortical cultures from ARE reporter mice revealed selective promoter activity in astrocytes. This activation protected neurons from hydrogen peroxide and nonexcitotoxic glutamate toxicity. tBHQ treatment of cultures from Nrf2 knock-out animals resulted in neither ARE activation nor neuroprotection. By reintroducing Nrf2 via infection with a replication-deficient adenovirus (ad), both the genetic response and neuroprotection were rescued. Conversely, infection with adenovirus encoding dominant-negative (DN) Nrf2 (ad-DN-Nrf2) or pretreatment with the selective phosphatidylinositol-3 kinase inhibitor LY294002 inhibited the tBHQ-mediated promoter response and corresponding neuroprotection. Interestingly, the adenoviral infection showed a high selectivity for astrocytes over neurons. In an attempt to reveal some of the cell type-specific changes resulting from ARE activation, cultures were infected with adenovirus encoding green fluorescent protein (GFP) (ad-GFP) or ad-DN-Nrf2 (containing GFP) before tBHQ treatment. A glia-enriched population of GFP-infected cells was then isolated from a population of uninfected neurons using cell-sorting technology. Microarray analysis was used to evaluate potential glial versus neuron-specific contributions to the neuroprotective effects of ARE activation and Nrf2 dependence. Strikingly, the change in neuronal gene expression after tBHQ treatment was dependent on Nrf2 activity in the astrocytes. This suggests that Nrf2-dependent genetic changes alter neuron–glia interactions resulting in neuroprotection.

Key words: **antioxidant response element; oxidative stress; neuroprotection; Nrf2; microarray; sulforaphane; glia–neuron interaction; cell sorting**

Introduction

The intraneuronal accumulation of reactive oxygen species has been implicated in the pathogenesis of many neurodegenerative diseases such as Alzheimer's, Parkinson's, and amyotrophic lateral sclerosis (Coyle and Puttfarcken, 1993; Simonian and Coyle, 1996; Mattson, 2000). The ability of a cell to neutralize reactive intermediates is, in part, dependent on the activation of a *cis*-acting regulatory element termed the antioxidant response element (ARE). The ARE is located in the 5′-flanking region of many genes essential for both detoxification and maintenance of cellular reducing potential (Rushmore et al., 1990, 1991). Thus, a powerful cluster of protective genes can be coordinately upregulated through the ARE to reduce the damage caused by harmful toxicants.

The functional characterization of the ARE sequence identified a core, TGACnnnGC, necessary for this transcriptional response (Rushmore et al., 1991). This finding led to the discovery of similar sequences in the promoter region of a growing list of neuroprotective genes that bind the transcription factor nuclear factor E2-related factor 2 (Nrf2) (Moi et al., 1994).

ARE induction by small-molecule activators such as *tert*-butylhydroquinone (tBHQ) has been shown to protect neuronal cell lines against the oxidative insult initiated by dopamine, hydrogen peroxide (H_2O_2), and glutamate (Murphy et al., 1991; Duffy et al., 1998; Li et al., 2002). This activation is dependent on the translocation of Nrf2 to the nucleus through inducer interaction with Keap1, the cytoplasmic repressor of Nrf2 (Dinkova-Kostova et al., 2002). In the nucleus, Nrf2 heterodimerizes with small Maf proteins before binding the ARE (Marini et al., 1997; Nguyen et al., 2000).

Received Aug. 15, 2003; revised Nov. 18, 2003; accepted Nov. 20, 2003.

This work was supported by Grants ES08089 (J.A.J.), ES10042 (J.A.J.), and ES09090 (Environmental Health Sciences Center) from the National Institute of Environmental Health Sciences. We thank Matthew Slattery and the Microarray Core Facility for conducting the gene array hybridizations; Kathy Schell and the Flow Cytometry Core Facility for cell sorting and technical assistance; Andy Shih and Dr. Tim Murphy for their assistance in the preparation of adenovirus; Dr. Albee Messing for GFAP–GFP mice; and Dr. Kaiman Chan and Dr. Yuet Wai Kan for Nrf2 KO mice. Special thanks to Jong-Min Lee for Nrf2 KO breeding partners; Thor Stein and Jiang Li for assistance with microarray data analyses; and Marcus Calkins, Julie Kern, Jon Kern, Jong-Min Lee, Jiang Li, Thor Stein, and Maria Spletter for intellectual and scientific input.

Correspondence should be addressed to Dr. Jeffrey A. Johnson, University of Wisconsin-Madison, 6125 Rennebohm Hall, School of Pharmacy, 777 Highland Avenue, Madison, WI 53705-2222. E-mail: jajohnson@pharmacy.wisc.edu.

DOI:10.1523/JNEUROSCI.3817-03.2004

 0270-6474/04/241101-12$15.00/0

Additional studies have shown that, in rodent primary neuronal cultures, both basal expression and activation of the ARE are seen predominately in the astrocyte, not neuronal, subpopulation (Ahlgren-Beckendorf et al., 1999; Eftekharpour et al., 2000; Murphy et al., 2001; Johnson et al., 2002). We speculate that this is attributable to selective Nrf2 expression in astrocytes over neurons (Shih et al., 2003). Our previous work has shown that Nrf2 overexpression in astrocytes can protect naive neurons (Shih et al., 2003), and that cortical neurons derived from Nrf2 knock-out (KO) mice have a heightened sensitivity to oxidative stressors (Lee et al., 2003b). These data suggest that activation of the Nrf2–ARE pathway in astrocytes confers protection to vulnerable neurons. The individual contributions of each cell type to this neuroprotection are yet to be defined.

To further elucidate the factors contributing to a protective response manifest by ARE activation, we used mouse primary cortical neuronal cultures to look at two paradigms of oxidative toxicity: H_2O_2 and glutamate. Cultures were made resistant to these toxicities through previous activation of the ARE by tBHQ and sulforaphane. The tBHQ-mediated protection was absent in Nrf2 KO cultures and inhibited by viral infection with dominant-negative (DN) Nrf2, as well as the phosphatidylinositol-3 (PI-3) kinase inhibitor LY294002 (LY). Lastly, the preferential adenoviral infection of glial cells in this mixed culture system was exploited, allowing us to use cell-sorting techniques to determine the cell type-specific, Nrf2-dependent genetic changes associated with tBHQ-mediated neuroprotection.

Materials and Methods

Animals. ARE–human placental alkaline phosphatase (hPAP) transgenic mice were created using 51 bp of the NAD(P)H:quinone oxidoreductase (NQO1) promoter upstream of a hPAP reporter construct (Johnson et al., 2002). Nrf2 KO mice were graciously provided by Drs. Kaiman Chan and Yuet Wai Kan (Howard Hughes Medical Institute, University of California, San Francisco, CA). The mice were created by replacement of the basic region-leucine zipper region with lacZ (Chan et al., 1996). Glial fibrillary acidic protein (GFAP)–green fluorescent protein (GFP) mice were a generous gift from Dr. Albee Messing (University of Wisconsin, Madison, WI). Green fluorescent protein (humanized GFP-S65T) was expressed under the control of the astrocyte-specific GFAP promoter (Zhuo et al., 1997). All of the ARE–hPAP mice were outbred onto C57B6/SJL mice (The Jackson Laboratory, Bar Harbor, ME) for experiments and thus were of mixed background.

Chemicals. Sulforaphane was purchased from LKT Labs (St. Paul, MN). All of the other chemicals were purchased from Fisher Scientific (Fair Lawn, NJ).

Mouse primary cortical cultures (modified from Hertz et al., 1985). On embryonic day 15 (E15), pregnant mothers were anesthetized with isoflurane and killed by cervical dislocation; pups were removed. The cortices were dissected and removed to HBSS. The tissue was dissociated with 0.05% trypsin in HBSS for 10 min at 37°C, and then filtered through a 70 μm cell strainer. Cells were plated on poly-D-lysine (PDL)-coated plates at $\sim 3.2 \times 10^5$ cells/cm^2 in CEMEM [10% fetal bovine serum, 10% horse serum, 2 mM L-glutamine, and 1% penicillin/streptomycin] for 45 min in a 37°C humidified tri-gas incubator (5% CO_2 and 5% O_2). For day 2 *in vitro* (2DIV) studies, treatments were performed after the initial 45 min incubation in CEMEM. For 5DIV studies, the cells were incubated in CEMEM for 48 hr before a medium change to Neurobasal medium (Invitrogen, Carlsbad, CA) with a B27 supplement containing antioxidants (NB plus AO) to specifically enhance neuronal growth. On the following day, the treatments were performed. Unless otherwise specified, after incubation with the treatment for 48 hr, the medium was changed to Neurobasal medium containing B27 supplement without antioxidants (NB minus AO) before the toxins were applied. This was done to prevent the direct interaction of the toxin with either the treatment or antioxidants such as catalase present in the medium.

Adenovirus. Recombinant adenovirus (ad) for enhanced GFP (eGFP) (ad-GFP), Nrf2-GFP (ad-Nrf2), and DN-Nrf2-GFP (ad-DN-Nrf2) were prepared, in collaboration with Dr. Tim Murphy at the University of Vancouver (Vancouver, British Columbia, Canada), by the Adenovirus Core Facility (Canadian Stroke Network Core Facility, University of Ottawa, Ottawa, Ontario, Canada). The Nrf2-cDNA was excised from the pEF/Nrf2 (Alam et al., 1999) using *Not*I and *Hin*dIII. These replication-deficient constructs were created using the Cre-lox system (Hardy et al., 1997) and were titered on human embryonic kidney 293 cells (Shih et al., 2003).

Treatments. All of the chemical pretreatments [vehicle is 0.005% ethanol (EtOH)] were added directly to the medium and were washed out in a medium change before toxin exposure. Cultures were incubated with replication-deficient adenovirus in MEM for 45 min at 37°C, after which the conditioned medium was added back to the cells.

Cytotoxicity. Forty-eight hours after treatments, cultures were incubated in either hydrogen peroxide or glutamate in fresh NB minus AO. On 5DIV, cells were incubated with H_2O_2 for 3 hr at 37°C. Catalase was added to the cultures at 105 U/ml to inactivate H_2O_2. Cultures were allowed to recover for 5 hr before a 3.5 hr quantification of cell viability using the Promega (Madison, WI) 3-(4,5-dimethylthiazol-2-yl)-5-(3-carboxymethoxyphenyl)-2-(4-sulfophenyl) 2H tetrazolium, inner salt (MTS) assay. For 2DIV cultures, cells were incubated with glutamate for 24 hr at 37°C before quantification of cell viability using the MTS assay.

Immunofluorescence. Primary antibodies were used at the following dilutions: anti-β(III)-tubulin, 1:200 (Promega); anti-GFAP, 1:1000 (Dako, Glostrup, Denmark); and anti-hPAP (clone 8B6), 1:400 (Sigma, St. Louis, MO). All of the secondary antibodies conjugated to either fluorescein or Texas Red were used at a dilution of 1:200, and appropriate IgG controls were run simultaneously. Terminal deoxynucleotidyl transferase-mediated biotinylated UTP nick end labeling (TUNEL) staining was performed using the Cell Death Detection kit from Roche (Indianapolis, IN) according to the manufacturer's instructions. Incubation of slides in Hoechst 33258 (0.1 mM in PBS; Sigma) was used to stain nuclear DNA. All of the images were taken using a Zeiss (Oberkochen, Germany) photomicroscope and analyzed using Axiovision software.

Immunofluorescence counts. Image fields (200×) were used to count cells displaying given immunofluorescent markers. Counts were expressed as percentage of vehicle to normalize for differences in cell density, immunostaining, and basal survivability variations across cultures. Cells displaying highly condensed nuclei, visible by bright spotting of Hoechst 33258 staining, were no longer considered viable and thus were not counted. GFAP-expressing cell counts had higher error values attributable to fewer cell numbers, as well as clustering of the cells beneath neurons, making exact counts difficult.

hPAP enzyme activity assay. Cells were harvested in TMNC lysis buffer (0.05 M Tris, 0.005 M $MgCl_2$, 0.1 M NaCl, 1% 3-[(3-cholamidopropyl)dimethylammonio]-1-propanesulfonate [CHAPS]) and freeze-thawed at −80°C. Endogenous phosphatase activity was heat inactivated at 65°C for 30 min in 0.2 M diethanolamine buffer. hPAP activity was quantitated by addition of the Applied Biosystems (Bedford, MA) substrates disodium 3-(4-methoxyspiro {1,2-dioxetane-3,2′-(5′-chloro) tricyclo [3.3.1.1 3,7]decan}-4-yl) phenyl phosphate and Emerald. A Berthold Orion microplate luminometer was used to measure the samples at various times after substrate addition. Values were corrected to an ARE–hPAP-negative culture and normalized by cell number at initial plating.

Total reduced glutathione assay (modified from Tietze, 1969). Cells were harvested in TMNC lysis buffer (0.05 M Tris, 0.005 M $MgCl_2$, 0.1 M NaCl, 1% CHAPS) and frozen at −80°C. Protein was precipitated from the lysates by mixing with an equal volume of 6% perchloric acid (PCA). Samples were spun at 7400 × *g* for 10 min at 4°C. The supernatant was diluted with 9 vols of 0.1 M sodium phosphate to neutralize the PCA. Reduced glutathione (GSH) standards and samples were further diluted six times with assay buffer (0.1 mg/ml dithionitrobenzoic acid and 0.32 mg/ml NADPH, in 0.1 M potassium phosphate). The reaction was started using 0.08 U of glutathione disulfide reductase per well of a 96 well plate. The absorbance was kinetically read at 410 nm, and the resulting values were corrected for protein via the BCA method (Pierce, Rockford, IL).

Reverse transcription-PCR. Cells were treated with tBHQ for 24 hr and harvested in TRIzol reagent (Invitrogen). After reverse transcription with oligo-dT primers using the Promega reverse transcription kit, the cDNA was probed using the following primers (IDT, Coralville, IA): β-actin (393 bp), 5′-tgttaccaactgggacgaca-3′ and 5′-ctctcagctgtggtggtgaa-3′; hPAP (351 bp), 5′-tgggtagctgggactacagg-3′ and 5′-ttgccccaaatctcaacttc-3′; Nrf2 (430 bp), 5′-aggcatcttgtttgggaatg-3′ and 5′-agttctcgctgctcggacta-3′; NQO1 (500 bp), 5′-ttcaaccccatcatttccag-3′ and 5′-tccagacgtttcttccatcc-3′; heme oxygenase-1 (HO-1) (603 bp), 5′-tacacatccaagccgagaat-3′ and 5′-gttcctctgtcagcatcacc-3′; and glutathione *S*-transferase (GST) μ1 (GSTm1) (450 bp), 5′-ctcccgactttgacagaagc-3′ and 5′-caggaagtccctcaggtttg-3′.

Specific-primed reverse transcription-PCR. The labeled amplified RNA (aRNA) isolated (see below) was used in a reverse transcription reaction with the specific sense (L) primers listed below rather than oligo primers. This cDNA was then analyzed in a PCR reaction with both the sense and antisense (L and R) primers listed below: β-actin (L), 5′-tgttaccaactgggacgaca-3′, and (R) 5′-ctctcagctgtggtggtgaa-3′; GFAP (L), 5′-ggagagggacaactttgcac-3′, and (R), 5′-gctctagggactcgttcgtg-3′; and β(III)-tubulin (L), 5′-gcttccagctgacacactca-3′, and (R), 5′-ttcttggcatcgaacatctg-3′.

Cell sorting. Littermate embryos were separately cultured as above into PDL-coated six well plates at two wells per embryo. After 2 d, the medium was changed to NB plus AO, and treatments were performed the following day. After incubation with the treatments for 24 hr, the cells were gently lifted with Accutase (US Biotechnologies, Parker Ford, PA) at 37°C for 20 min, spun down at 300 × *g* for 2 min, and resuspended in diethylpyrocarbonate (DEPC)–PBS with 1% BSA. Samples were kept on ice and filtered through a 41 μm strainer before sorting to remove large aggregates. Cells were sorted using a FACSVantage SE equipped with FACS DiVa option into carrier solution (DEPC–PBS with BSA). To sort, cells were excited with a 488 nm argon laser at 100 mW, and GFP emission was collected through a 530/30 bandpass filter. The populations were sorted from viable cells [using forward scatter (FSC)/side scatter (SSC) size dimensions to discard debris] that did not display potential double characteristics (FSC-width windows). In addition, in an attempt to get solely GFP-expressing cells in one pool and completely GFP-negative cells in another, a third pool with low fluorescence was collected and discarded [fluorescence detector 1 (FL1)-GFP from ~5 to 25] (see Fig. 7). The sorted populations were spun at 300 × *g* for 2 min, resuspended in TRIzol reagent (<0.25 ml per 50,000 cells), and stored at −80°C before RNA isolation. A sort check after the separation indicated >99.9% purity in the GFP-negative pool and >95% purity in the GFP-positive pool [using propidium iodide (PI), the outlying 5% in the GFP-positive pool revealed a significant percentage of dead cells that were swollen and/or had some autofluorescence; it should be noted that the RNA from these compromised cells would be quickly degraded and eliminated from additional isolation steps].

GeneChip analysis. E15 individual primary cultures were grown in CEMEM for 2DIV before changing the medium to NB plus AO. On the subsequent day, cultures were infected with either 50 multiplicity of infection (MOI) ad-GFP or ad-DN-Nrf2 for 45 min in MEM. After replacement of the conditioned medium, the cultures were treated with vehicle or 10 μM tBHQ. Twenty-four hours later, cells were lifted using Accutase and sorted in single-cell suspensions, resuspended in TRIzol, and frozen at −80°C. RNA was isolated from TRIzol following the Invitrogen protocol for RNA isolation. Double-stranded cDNA was synthesized from the RNA according to the Ambion (Austin, TX) protocol for use of their MessageAmp aRNA kit; purified using glycogen, ethanol, and ammonium acetate; and then *in vitro* transcribed to aRNA using the Ambion T7 ribonucleotides. The aRNA was purified, and the samples were reverse transcribed back to cDNA using second-round primers. A second round of *in vitro* transcriptional amplification to aRNA was performed, this time using the Enzo (Farmingdale, NY) biotin-labeled ribonucleotides at a final concentration of 7.5 mM. The end product was purified using Qiagen (Valencia, CA) RNeasy columns. The concentration and quality of the labeled aRNA were assessed, and 15 μg of fragmented aRNA was hybridized for 16 hr at 45°C to a murine U74Av2 array (Affymetrix, Santa Clara, CA). The arrays were automatically washed and stained with streptavidin–phycoerythrin using a fluidics station. Last, probe arrays were scanned at 3 μm resolution using the Genechip System confocal scanner made for Affymetrix by Agilent. Affymetrix Microarray Suite 5.0 was used to determine the relative intensities of each gene and the corresponding treatment comparisons. Intensity readings were scaled to a constant value (scale factor). To determine the rank of the changed genes, two intergroup comparisons (2 × 2 matrix) were performed based on the change called (0, no change; 1/−1, marginal increase/marginal decrease; 2/−2, increase/decrease). The sum of these four difference calls gave the final rank. The ranks varied from −8 to 8, and values were cut off at −4/4. Analysis parameters were set at $\gamma 1 = 0.01$ and $\gamma 2 = 0.05$; thus, ranks of −8/8 and −4/4 approximate $p < 0.01$ and $p < 0.05$, respectively. To increase the stringency of the analysis, genes with a coefficient of variation (CV) of >1.0 were eliminated[a] (Li and Johnson, 2002). In addition, a value of 1.5 for average fold change (FC) was set as the cutoff for increased genes, and decreased genes below −3-fold are shown[a] (note that some genes ranked 4/−4 may be omitted for reasons of space; see supplementary tables for a complete listing at http://www.pharmacy.wisc.edu/facstaff/sciences/JohnsonGroup/microdata.cfm).

To achieve a list of potential neuronal versus astrocyte markers, only those genes with a rank of 8 from a 2 × 2 comparison of the GFP vehicle-positive and -negative pools were considered. These genes with FC greater than threefold and CV of <1.0 were then analyzed against a single comparison ($n = 1$) of populations from a set of sorted cultures derived from GFAP-driven GFP transgenic mice. Only those genes ranking 8 from the 2 × 2 comparison that were also appropriately called increased or decreased from the GFAP–GFP cultures were chosen to demonstrate potential cell type-specific markers in this culture system.

Supplementary material. Additional data for this article are available online at http://www.pharmacy.wisc.edu/facstaff/sciences/JohnsonGroup/microdata.cfm.

Results

tBHQ and sulforaphane activate the ARE in astrocytes

Cells derived from animals expressing the ARE–hPAP transgene (Johnson et al., 2002) were evaluated for hPAP expression 48 hr after treatment with either tBHQ or sulforaphane. Both tBHQ (Fig. 1*A*) and sulforaphane (*B*) induced a dramatic, dose-dependent increase in hPAP activity. The mRNA levels for ARE-driven hPAP, Nrf2-dependent GSTm1 (Chanas et al., 2002), and other ARE-dependent genes (Fig. 1*C*), as well as total GSH levels (*D*), were correspondingly increased in the cortical neuronal cultures.

tBHQ has been shown previously to activate the ARE in the astrocyte subpopulation rather than neurons using analyses of either ARE-responsive genes such as NQO1 and GSTp1 (GST π1) (Ahlgren-Beckendorf et al., 1999) or an hPAP reporter construct (Murphy et al., 2001; Johnson et al., 2002) (data not shown). Immunofluorescence staining using an antibody to the hPAP protein (Texas Red) in conjunction with an antibody to the astrocyte marker GFAP (FITC) demonstrated a large increase in the presence of hPAP protein in GFAP-positive cells displaying astrocytic morphology (flattened with large cell bodies) after treatment with tBHQ (data not shown) or sulforaphane (Fig. 1*E*, arrows). Very few cells displaying neuronal morphology exhibited increased hPAP protein. Although all of the astrocytes visible in the sulforaphane-treated fields are not expressing the hPAP reporter protein, the majority of them are likely ARE activated. This reflects the fact that mixed embryos (+/− and −/− for the transgene because of breeding +/− males to −/− females) were used to generate these cultures; therefore, not all of the cells contain the hPAP transgene. In addition, chemicals structurally re-

[a]For genes of interest with FC or CV outside of these cutoffs, the outlying values are shown in bold. Special consideration should be paid to the lower-ranked genes with a high CV (>1.0), low basal expression (baseline signal, <300), or small fold change (<2) because of the potential for bias from two rounds of amplification.

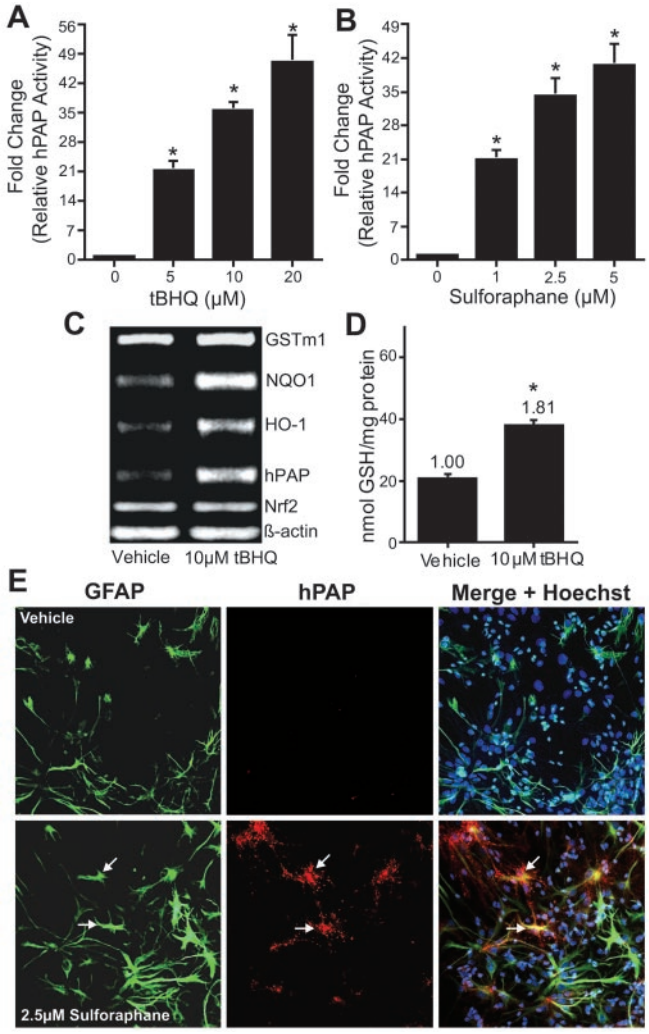

Figure 1. ARE activity in mixed (neurons and glia) cortical cultures after treatment with tBHQ or sulforaphane. *A*, *B*, Fold change indicating the relative conversion of an hPAP substrate in cortical cultures derived from transgenic animals containing an hPAP reporter construct under the control of 41 bp of the NQO1 promoter containing the ARE sequence. Cultures were treated with tBHQ (*A*) or sulforaphane (*B*) for 48 hr before an enzyme assay for hPAP activity. Cultures from animals negative for the ARE– hPAP transgene were used to subtract background luminescence. Values indicate the fold increase in ARE-driven hPAP substrate conversion compared with vehicle ($n = 4$; mean ± SE; $^*p < 0.05$). *C*, RT-PCR of RNA isolated from ARE– hPAP cultures treated with 10 μM tBHQ for 24 hr. Treated cultures were assessed for the presence of increased mRNA of known ARE-dependent genes [GSTm1, HO-1, NQO1, hPAP (reporter gene), β-actin (internal control)]. *D*, Total intracellular glutathione was determined for individual, mixed primary cultures treated with either 10 μM tBHQ or vehicle (0.005% EtOH) for 48 hr ($n = 3$; mean ± SE; $^*p < 0.05$). GSH, Total intracellular glutathione (reduced form). *E*, Immunofluorescence staining of ARE– hPAP cultures 48 hr after treatment with 2.5 μM sulforaphane (bottom panels) versus vehicle (top panels). Anti-hPAP antibody is shown as punctate red staining (Texas Red) and anti-GFAP is green (FITC). The majority of cells displaying hPAP protein have GFAP-positive processes or GFAP staining overlaid with hPAP fluorescence (arrows). Small cells stained with Hoechst 33258 (blue) that do not display GFAP staining are likely neurons.

lated to tBHQ such as butylated hydroxyanisole (–OCH_3 in 4′ position instead of –OH) and di-*tert*-butylhydroquinone (additional *tert*-butyl group in the 5′ position) did not increase activation of the ARE as determined by hPAP enzymatic activity (data not shown).

tBHQ and sulforaphane pretreatment protects against oxidative stress-induced death in neurons

To determine whether these small-molecule inducers of the ARE can protect cells against oxidative stress, cultures were exposed to hydrogen peroxide (Fig. 2) and glutamate (Fig. 3). H_2O_2-induced cellular toxicity is characterized by a depletion of intracellular glutathione (GSH) and ATP, increased Ca^{2+} levels, and lipid peroxidation (Fernandez-Checa et al., 1997; Li et al., 1997). Oxidative glutamate toxicity results in high levels of extracellular glutamate that competitively inhibits the uptake of cystine by immature neural cells via the system x_c^- [cystine transporter (xCT)] (Murphy et al., 1989, 1990). The subsequent decrease in intracellular concentrations of cysteine results in lowered GSH levels and NMDA receptor-independent cell death, presumably because of the accumulation of free radicals. It is very important to note that all of the cytotoxicity experiments were performed in fresh medium (NB minus AO), and that both tBHQ and sulforaphane were not present in the medium with H_2O_2 or glutamate. This was done in an effort to examine the changes in gene expression rather than any direct antioxidant properties the treatments may possess. As observed by immunofluorescent staining, tBHQ pretreatment for 48 hr showed a remarkable attenuation of cytotoxicity induced by H_2O_2 (Fig. 2*A–C*). Sulforaphane was just as effective as tBHQ at blocking this cytotoxicity (Fig. 2*D*). Actual cell counts of the fluorescent-stained cultures support the visual observation that tBHQ or sulforaphane can protect these cells from H_2O_2-induced cytotoxicity. By setting vehicle-treated images at 100% ($n = 8$), it was determined that 50 μM H_2O_2 significantly decreased the total cells (Hoechst; $n = 6$) present to 20.7 ± 3.90% of vehicle. Within the cell subpopulations, this correlated to a significant decrease in neuronal [β(III)-tubulin; $n = 6$] viability to 4.30 ± 1.40% of vehicle and astrocytes (GFAP; $n = 6$) to 59.9 ± 20.7% of vehicle. Pretreatment with 10 μM tBHQ ($n = 8$) significantly attenuated the total cell death (81.2 ± 6.30%), the neuron-specific death (53.0 ± 6.80%), and the astrocytic death (86.7 ± 9.00%) caused by treatment with H_2O_2. Pretreatment with 2.5 μM sulforaphane ($n = 4$) resulted in similar protection against H_2O_2-induced cytotoxicity [Hoechst, 115 ± 11.6%; β(III)-tubulin, 76.5 ± 10.8%; and GFAP, 111 ± 13.7% of vehicle]. Interestingly, cell death induced by hydrogen peroxide was more selective for neurons than astrocytes at the doses used. Pretreatment of mixed cultures with tBHQ or sulforaphane exhibited a pattern of increased GFAP-positive and β(III)-tubulin-positive cells, indicating an enhanced survival of astrocytes and neurons, respectively. In addition, hydrogen peroxide leads to an increase in TUNEL-positive cells that was also attenuated by tBHQ pretreatment (data not shown). Furthermore, the overall cell viability, as measured by the MTS assay, of cultures exposed to increasing doses of H_2O_2 was enhanced when pretreated with 10 μM tBHQ for 48 hr (Fig. 2*E*). Previous studies have implicated PI-3 kinase in ARE activation by tBHQ (Lee et al., 2001; Johnson et al., 2002; Kang et al., 2002). Hence, we pretreated cultures with the PI-3 kinase inhibitor LY for 30 min before tBHQ treatment. Indeed, LY pretreatment blocked both the activation of the ARE promoter, similar to that seen previously (Johnson et al., 2002) (data not shown), and inhibited the tBHQ-induced protection against hydrogen peroxide (Fig. 2*F*).

Similar results to that described above were observed with respect to glutamate-induced cytotoxicity. Cell viability (Fig. 3*A*), immunofluorescent staining (*B–D*), and cell counts of cultures pretreated with 10 μM tBHQ (or 2.5 μM sulforaphane) (data not shown) before glutamate exposure, demonstrated similar survival characteristics. In addition, TUNEL-positive cells were dramatically decreased in cultures pretreated with tBHQ before glutamate exposure (Fig. 3*E–H*). Immunofluorescent counts reflected the visual observations in that only 28.6 ± 0.80% of the Hoechst-stained cells and 7.70 ± 1.20% of the β(III)-tubulin-

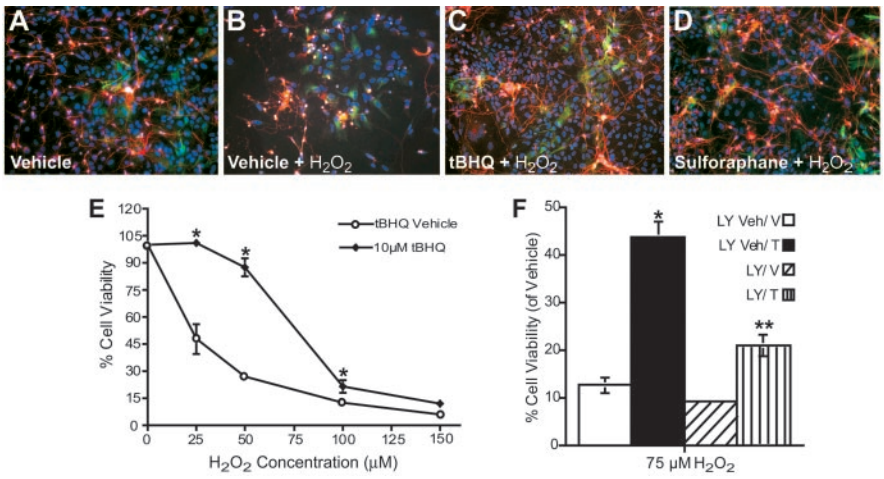

Figure 2. tBHQ-mediated attenuation of H_2O_2-induced cell death and loss of protection by inhibition of PI-3 kinase. *A–D*, Cells were pretreated with vehicle (*A* and *B*), 10 μM tBHQ (*C*), or 2.5 μM sulforaphane (*D*) for 48 hr before 50 μM H_2O_2 treatment (*B–D*). *A*, Hydrogen peroxide vehicle (PBS) treatment is represented. Neurons are indicated by red staining for β(III)-tubulin and astrocytes are shown in green (GFAP). The nuclear counterstain (Hoechst 33258; blue) shows condensed (bright) and fragmented DNA in apoptotic cells (magnification, 200×). *E*, 5DIV cultures pretreated for 48 hr with 10 μM tBHQ were exposed to a 3 hr incubation with hydrogen peroxide. Cell viability was assessed using the soluble MTS assay ($n = 4$; mean ± SE; $^*p < 0.05$, compared with vehicle). Error bars indicate mean ± SEM for four experiments. *F*, ARE– hPAP cultures were pretreated for 30 min with the PI-3 kinase inhibitor LY (10 μM) before a 10 μM tBHQ (T) treatment. H_2O_2 cytotoxicity at 75 μM was used 48 hr after tBHQ treatment to observe the effect of LY pretreatment on tBHQ-mediated neuroprotection (LY, 10 μM LY294002; LY Veh, LY vehicle, 0.01% DMSO; T, 10 μM tBHQ; V, tBHQ vehicle, 0.005% EtOH; $n = 3$; $^*p < 0.05$, compared with LY Veh/H_2O_2 vehicle; $^{**}p < 0.05$, compared with LY Veh/H_2O_2 vehicle and compared with LY vehicle/tBHQ with 75 μM H_2O_2). Error bars indicate mean ± SEM for three experiments.

positive cells remained after 1 mM glutamate treatment ($n = 4$). Pretreatment with 10 μM tBHQ ($n = 4$) resulted in a significantly enhanced viability of both total cells and neurons to 75.9 ± 3.90% and 67.8 ± 3.90% of vehicle controls, respectively, when a 1 mM glutamate insult was applied. In addition, pretreatment with tBHQ resulted in marked attenuation of TUNEL-positive cell counts (percentages expressed as TUNEL-positive cells divided by total, Hoechst-stained nuclei). Whereas vehicle pretreatment resulted in 58.4 ± 4.90% of the cells displaying fragmented DNA after 1 mM glutamate insult, tBHQ-pretreated cultures exhibited only 13.8 ± 4.20% (glutamate vehicle treatment resulted in 4.80 ± 1.80% TUNEL positive; $n = 3$).

To ensure that the oxidative glutamate toxicity was indeed oxidative stress induced and not a result of NMDA receptor-induced excitotoxicity, cultures were pretreated with 100 μM *N*-acetyl-L-cysteine (NAC). NAC provides cells with an alternative form of cysteine for GSH synthesis by circumventing the xCT. Pretreatment with NAC showed a complete block of glutamate-induced cellular death, whereas the synthetic NMDA receptor inhibitor MK-801 did not block cell death (data not shown).

ARE activation and protection against oxidative stress are dependent on Nrf2

The induction of genes in response to tBHQ has been shown to be dependent on binding of the transcription factor Nrf2 to the ARE core sequence (Lee et al., 2003a). To look at the dependence on Nrf2 in a mixed culture of astrocytes and neurons, we prepared cultures from ARE–hPAP × Nrf2 KO mice (Chan et al., 1996). Nrf2 knock-out mice have a heightened sensitivity to oxidative stress, including an increased susceptibility to carcinogenesis (Ramos-Gomez et al., 2001). In these cultures, tBHQ was unable to induce ARE activity (data not shown), exhibited no protection versus hydrogen peroxide (Fig. 4*A*) (note: KO cells are a bit more sensitive to H_2O_2) or glutamate (data not shown), and displayed no enhancement of β(III)-tubulin-positive cell survival after hydrogen peroxide treatment (Fig. 4*B*). Immunofluorescence cell counts revealed 20.8 ± 3.90% versus 27.2 ± 4.60% total (Hoechst-stained) cell survival after a 50 μM H_2O_2 insult subsequent to pretreatment with vehicle or 10 μM tBHQ, respectively. Neuronal survivability after insult was also unchanged (vehicle pretreatment, 3.2 ± 1.3%, and tBHQ, 2.6 ± 0.9% of H_2O_2 vehicle controls). It should be noted that tBHQ treatment alone resulted in no significant cell count changes from those seen with vehicle treatment ($n = 4$).

Overexpression of Nrf2 restores neuroprotection and ARE activity

In an effort to further establish that Nrf2 is necessary for protection, knock-out cultures were infected with replication-deficient adenovirus encoding Nrf2 (ad-Nrf2). An MOI (plaque-forming units per cell) of 50 resulted in a near-complete protection of the cultures against hydrogen peroxide (Fig. 5*A*) or glutamate (data not shown). Ad-Nrf2 infection also resulted in an increase in ARE reporter activation as seen by immunofluorescent staining as well as hPAP enzyme activity (Fig. 5*B*,*D*). This correlated with a significantly increased survivability of β(III)-tubulin-positive cells (Fig. 5*C*). Immunofluorescence counts indicate 3.1 ± 1.7% survival of β(III)-tubulin positive cells infected with ad-GFP after insult, whereas infection with 50 MOI of ad-Nrf2 completely protected the neurons from glutamate toxicity (survival, 94.1 ± 4.3%). Cytotoxicity appears to be selective for neurons, because staining for β(III)-tubulin is drastically decreased in unprotected cultures (Fig. 5*C*) (in 0 and 50 MOI GFP-infected cultures treated with H_2O_2). Lastly, overexpression of Nrf2 resulted in an increase in total intracellular GSH levels (Fig. 5*E*) similar to that seen with tBHQ treatment (Fig. 1*D*).

Introduction of DN-Nrf2 to wild-type cultures results in a decrease in tBHQ-mediated cellular protection and ARE activation

To determine the endogenous contributions of Nrf2 to tBHQ-mediated events, cortical cultures from ARE–hPAP mice were infected with ad-DN-Nrf2 before tBHQ treatment. This mutant lacks the N-terminal transcription activation domain, but still retains the C-terminal DNA binding and heterodimerization domain. It is thought to inhibit Nrf2 by competing with the transcription factor for binding partners and/or DNA binding sites (Alam et al., 1999). Interestingly, when primary cortical cultures were injected with low concentrations of adenovirus (<75 MOI), it appeared that the viral infection was selective for astrocytic cell types (Fig. 6*A*,*B*). Therefore, low concentrations of the adenovirus were used to selectively infect the astrocytes in this mixed-culture system. Infection of astrocytes with ad-DN-Nrf2 before tBHQ treatment resulted in a large attenuation of tBHQ-mediated activation of the ARE response (Fig. 6*C*). Amazingly, this also led to a reversal of the tBHQ-mediated neuroprotection

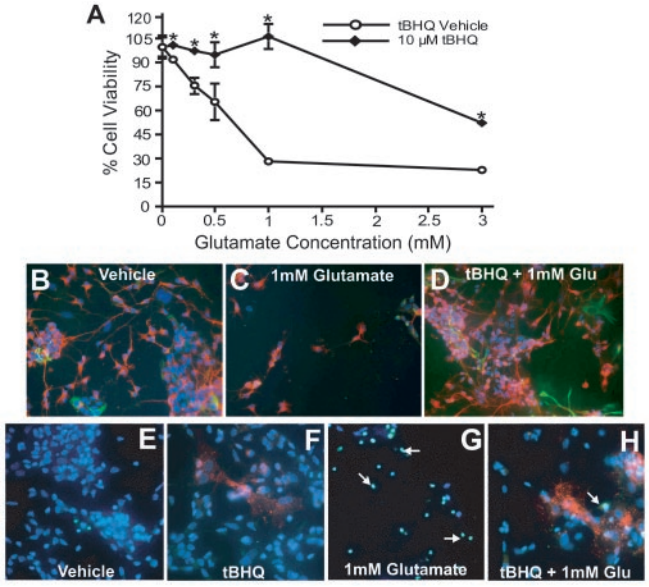

Figure 3. tBHQ-mediated attenuation of glutamate-induced cell death. *A*, 2DIV cultures were incubated with a high extracellular concentration of glutamate for 24 hr after a 48 hr pretreatment with either 10 μM tBHQ or ethanol vehicle (*$p < 0.05$; $n = 4$; mean ± SE). Cell viability was assessed using the soluble MTS assay. *B–D*, Oxidative glutamate (Glu) (1 mM) toxicity after a 48 hr treatment with vehicle (*C*) or 10 μM tBHQ (*D*). Error bars indicate mean ± SEM for four experiments. *B*, Cells after treatment with glutamate vehicle (double distilled H_2O) are shown. β(III)-tubulin (red) indicates the remaining neurons and GFAP (green), the scattered astrocytes (magnification, 400×). *E–H*, TUNEL stain of cells displaying fragmented DNA (bright green; arrows) overlaid with Hoechst 33258 (blue) and anti-hPAP antibody (red) immunofluorescence 24 hr after treatment with glutamate vehicle (*E*, *F*) or 1 mM glutamate (*G*, *H*) pretreated for 48 hr with tBHQ vehicle (*E*, *G*) or 10 μM tBHQ (*F*, *H*) (magnification, 400×). Note: *B–D* represent a separate culture from *E–H*.

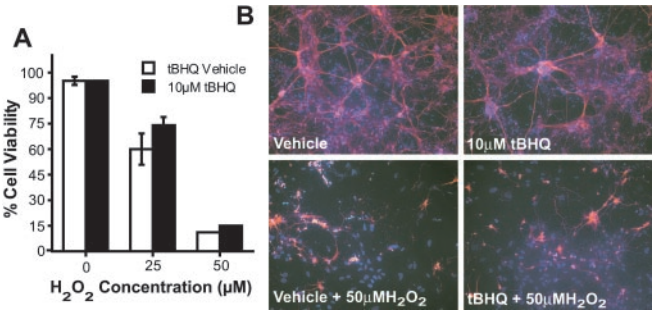

Figure 4. In Nrf2 KO cultures, in which the effect of tBHQ on ARE activity is lost, neuronal protection is abrogated. *A*, Pretreatment of Nrf2 KO cultures with 10 μM tBHQ and vehicle for 48 hr was performed before H_2O_2 treatment. Error bars indicate mean ± SEM for four experiments. *B*, KO cultures were treated with 10 μM tBHQ or vehicle for 48 hr before a 50 μM insult of H_2O_2. Cultures were then stained for β(III)-tubulin (red) to qualify the presence of neurons and Hoechst 33258 (blue) to indicate additional cell types remaining, as well as apoptotic cells (displaying condensed or fragmented nuclei; magnification, 200×).

against hydrogen peroxide-induced cytotoxicity (Fig. 6*D*). Knowing that ARE activation by tBHQ occurs predominately in the astrocyte subpopulation, ad-DN-Nrf2 preferentially infects astrocytes, and neurons are more susceptible than astrocytes to H_2O_2-induced toxicity, these data suggest that ARE activation in astrocytes confers protection to vulnerable neurons (compared with ad-GFP controls).

FACS cell sorting of adenovirus-infected cultures

To elucidate phenotypic characteristics of the sorted cell populations to be used for oligonucleotide microarray analysis of mRNA levels, size and fluorescence data gained during gating of the populations were evaluated. Individual primary cultures from ARE–hPAP mice were treated on 3DIV with either ad-GFP or ad-DN-Nrf2 virus followed by tBHQ or vehicle. Twenty-four hours later, cells were sorted on a FACSVantage SE cell sorter. A representative example of the sort gates and cell populations is given in Figure 7. GFP gates were stringently set, discarding a population with low fluorescence between sorted populations of no fluorescence and high fluorescence. Additionally, doublets (clumps of cells; larger FSC width) were discarded because of the potential for GFP-negative cells in GFP-positive clusters. Normally, between 60 and 70% of the total cells were sorted (Fig. 7*A*, R1 population), eliminating debris and dead cells from subsequent RNA isolation steps. Of these viable cells, on average, 15% were sorted into the GFP-positive pool (R3) and 60% into the GFP-negative pool (R4), eliminating ~30% (from R2) because of indeterminate fluorescence or clumping. It was noted during sorting that two populations of different sizes were present, correlating with the GFP-infected versus -uninfected populations (Fig. 7*C*, R3 vs R4). Average cell size was analyzed using the *X* and *Y* mean values generated from the FSC (a measurement of cell size) versus SSC (a measurement of granularity or cell complexity) parameters. It was noted that the GFP-positive populations had average *X* and *Y* means of 411.9 ± 4.2 and 371.4 ± 10.8, respectively, whereas the GFP-negative populations had values of 202.3 ± 5.7 and 126.0 ± 6.8 ($n = 8$). Astrocytes in culture appear to occupy larger volumes than neurons. Accordingly, this large difference in cell size between sorted populations may be attributed to the preferential uptake of adenovirus by astrocytes versus neurons. Postsort checks of the isolated populations showed <0.01% contamination in the GFP-negative pool and <5% contamination in the GFP positive (likely dead cells exhibiting autofluorescence). By separating specific cell subpopulations, this powerful tool can be used to elucidate cell type-specific markers (neurons vs glia) as well as the cell-specific genetic alterations induced by tBHQ treatment.

Identification of cell type-specific markers in the sorted cell populations

To verify that the cRNA maintained a qualitative differential between astrocytes and neurons, total RNA was amplified and biotinylated cRNA was generated for each of the GFP-positive (primarily astrocytes) and GFP-negative (neurons) sorted populations that were described above. Reverse transcription-PCR (RT-PCR) for GFAP and β(III)-tubulin was performed on the biotinylated cRNA (Fig. 7*G*). Indeed, there was a clear absence of GFAP when compared with β(III)-tubulin in the GFP-negative cells and a slight carryover of β(III)-tubulin in the GFP-positive sorted pool. This set of samples and an independently derived second set of sorted samples were then subjected to microarray analysis.

To determine transcripts expressed at much higher levels in astrocytes than in neurons and vice versa, a 2 × 2 matrix analysis comparing GFP-positive (vehicle-treated) with GFP-negative (vehicle-treated) was performed. A third sort from cultures derived from GFAP-driven GFP mice was used to verify the astrocyte-specific gene list, in that the GFP-positive sort from these cultures had a >99% similar size and represented a pure astrocyte subpopulation. Thus, genes with a rank of 8/−8 and a fold change of ≥3/less than or equal to −3, that passed CV (CV ≤ 1) and also were appropriately called increased or decreased in the comparison from the GFAP–GFP sort, are indicated as neuron or astrocyte specific (Table 1). Although some genes do not

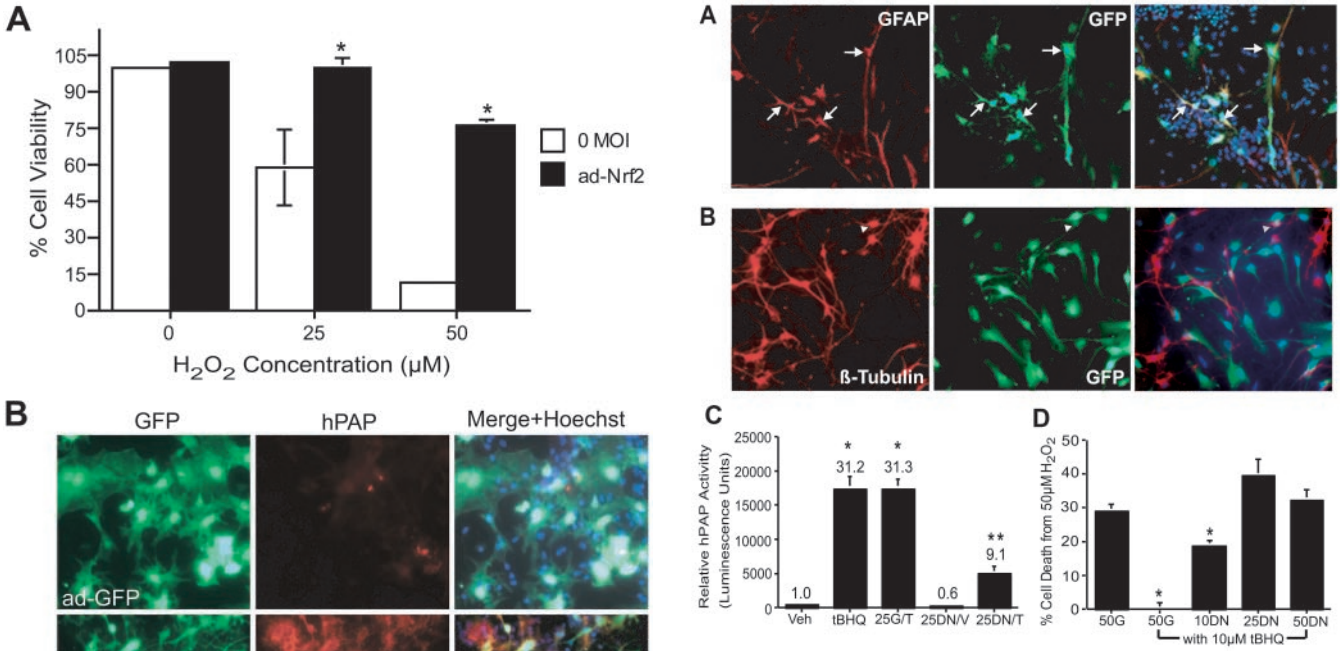

Figure 5. Overexpression of Nrf2 resulting in ARE activation and neuroprotection. *A*, Nrf2 KO cultures were infected with 50 MOI ad-Nrf2 48 hr before H_2O_2 insult. ($n = 4$; $^*p < 0.05$). *B*, ad-GFP- and ad-Nrf2-GFP (50 MOI)-infected cultures were observed for ARE activation in primary cultures from ARE– hPAP transgenics using hPAP antibody staining [hPAP antibody (red); eGFP fluorescence (green); Hoechst 33258 (blue); magnification, 400×]. *C*, Staining for the neuronal marker, β(III)-tubulin (red), after a 50 μM insult with H_2O_2 [eGFP (green); Hoechst 3258 (blue); 0 MOI, no virus/MEM alone; magnification, 400×]. *D*, *E*, Forty-eight hours after treatment with 50 MOI ad-GFP or 50 MOI ad-Nrf2, ARE– hPAP cultures were harvested in lysis buffer and evaluated for hPAP enzyme activity (*D*) and total glutathione (*E*) (50 GFP, 50 MOI ad-GFP; 50 Nrf2, 50 MOI ad-Nrf2). GSH concentration (*E*) was corrected for protein using the BCA method ($n = 4$; mean ± SE; $^*p < 0.05$). Error bars in *A*, *D*, and *E* indicate mean ± SEM for four experiments.

Figure 6. Selective adenovirus infection of astrocytes leads to ad-DN-Nrf2-mediated reduction in ARE activation by tBHQ and inhibition of tBHQ-mediated neuroprotection. Infection of primary cortical cultures with with low MOIs (25–75) of adenovirus show ad-infected cells colocalized with GFAP-positive astrocytes (*B*, arrows) (50 MOI; magnification, 200×) and, very infrequently, β(III)-tubulin-positive neurons (*C*, arrowheads) (75 MOI; magnification, 400×). On 3DIV, ARE– hPAP cultures were infected with ad-DN-Nrf2 (DN) virus or ad-GFP (G) virus (25 or 50 MOI) for 45 min, followed by treatment with 10 μM tBHQ or tBHQ vehicle. *C*, ARE activation by tBHQ was quantified by conversion of an hPAP substrate to a luminescent product (fold change of vehicle is shown above each bar; $n = 5$; mean ± SE; $^*p < 0.05$, significant increase compared with vehicle; $^{**}p < 0.05$, significant increase compared with vehicle and significant decrease compared with 25 MOI ad-GFP + 10 μM tBHQ). Veh, Vehicle; T, 10 μM tBHQ; V, vehicle. *D*, Cytotoxicity caused by 50 μM H_2O_2 was calculated using the MTS viability assay. The percentage of cell death induced in the presence of 50 MOI ad-GFP with tBHQ vehicle or 10 μM tBHQ (50 G/Veh and 50 G/T, respectively), was compared with the cell death induced in the presence of 10, 25, and 50 MOI of the DN-Nrf2 adenovirus with 10 μM tBHQ ($n = 3$; mean ± SE; $^*p < 0.05$, significant attenuation of cell death compared with 50 MOI GFP: vehicle-treated cultures exposed to 50 μM H_2O_2). Error bars in *C* and *D* indicate mean ± SEM for three experiments.

appear to be common cell-specific markers, the majority have previously been shown to be transcribed specifically in either neurons or astrocytes. The tubulins, stathmins, and synaptosomal-associated proteins have been associated with neurons, whereas genes such as Nfe2l2, phosphoprotein enriched in astrocytes 15, and GSTm1 are expressed at much higher levels in astrocytes.

Identification of Nrf2-dependent tBHQ-induced genetic changes in sorted cell populations

To determine potential cell-specific contributions to ARE activation and Nrf2-dependent neuroprotection induced by tBHQ,

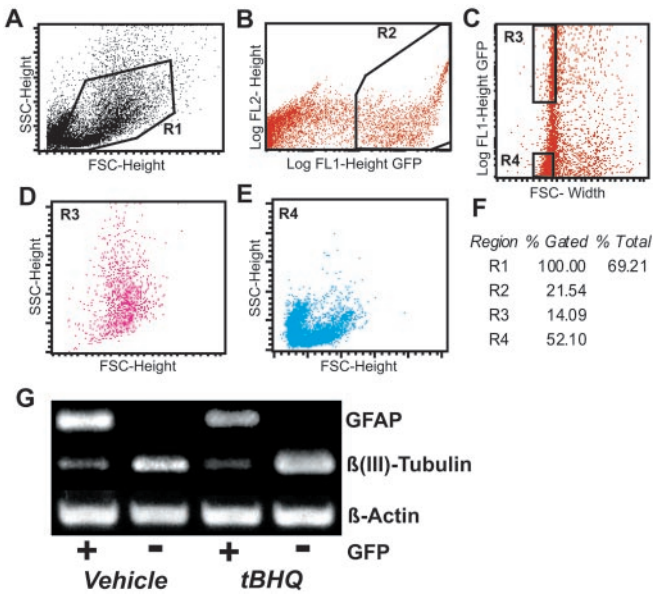

Figure 7. Cell sorting of adenovirus-infected cultures reveals two distinctly sized populations, correlating to an astrocyte-enriched versus a neuronal population. 3DIV cultures were infected with adenovirus encoding either GFP (ad-GFP) or DN-Nrf2-GFP (ad-DN-Nrf2) and treated with 10 μM tBHQ or vehicle for 24 hr. Cells were lifted with Accutase, filtered, and sorted according to their GFP content (indicating viral infection). *A*, The first sort gate was used to determine that ~69% of the total population were deemed to be healthy cells free of debris according to size (*F*, R1). All of the subsequent gates were set on R1 so that only viable cells were analyzed and sorted. *B*, R2 shows the viable cell fluorescence for GFP (FL1, *x*-axis). The *y*-axis (FL2) is a measure of the orange fluorescence, because very strong GFP fluorescence can emit orange. These axes were used during postsort checks to compensate for dead cells that take up PI versus GFP fluorescence. R2 indicates that ~21% of the viable cells were considered GFP-positive, and 79% were considered negative (see *F*). These, however, were not the final populations used to represent the GFP-positive and -negative populations. In *C*, the viable cells (R1) were gated for GFP fluorescence along the *y*-axis, but also for width along the *x*-axis (to remove doublets or clumps of cells from the sort that, potentially, could contain both GFP-positive and -negative cells). Thus, R3 represents the GFP-positive population isolated, and R4 represents the GFP negative [note that a large window was left between R3 and R4 in an attempt to get highly pure populations, eliminating cells with medium fluorescence (*y*-axis)]. Of the viable cells, the GFP-positive population was ~14%, and the GFP-negative population was ~52% (*C*; *F*, R3 and R4). *D*, The size of the cells isolated as the GFP-positive pool of cells is shown. *E*, The size of cells isolated as the GFP-negative population is indicated. Larger cells have higher FSC-height and/or higher SSC-height values (R3 cell size > R4 cell size). *G*, Mixed wild-type cultures were infected with 50 MOI ad-GFP on 3DIV and treated with tBHQ vehicle or 10 μM tBHQ 24 hr before cell sorting. Amplified RNA isolated from GFP-positive (+) and GFP-negative (−) sorted cell populations was then subjected to specific-primed reverse transcription with the sense primers for GFAP, β(III)-tubulin, and β-actin (internal control). PCR was then run on the samples using 3′ and 5′ primers. GFP-positive (+) populations (adenovirus-infected cells) from either tBHQ- or vehicle-treated cultures have transcripts highly enriched for the glial marker, GFAP, when compared with the neuronal marker, β(III)-tubulin. The GFP-negative (−) populations (uninfected) are nearly entirely made up of transcripts for the neuronal marker, β(III)-tubulin, with minimal to no expression of GFAP.

cells were infected with 50 MOI ad-GFP or ad-DN-Nrf2 and treated with tBHQ. The ensuing cell sort resulted in the production of an astrocyte-enriched (>85% astrocytes) GFP-positive population and a nearly pure neuronal (>99% neuron) GFP-negative population. Analysis of the mRNA representing these populations revealed that there was little overlap of genes changed by tBHQ treatment in both the astrocyte-enriched and neuronal populations. Of the 97 genes increased in the astrocyte-enriched population, only 4 were also increased in neurons. Similarly, only 9 genes were decreased in both the astrocyte-enriched and neuronal populations. In addition, ad-DN-Nrf2 blocked or significantly inhibited 80 of the 97 increased genes, as well as

Table 1. Gene changes in neuronal versus astrocyte-enriched sorted populations

Cell type markers	Fold	Gene name
Neuronal markers	32.9	Distalless homeobox 1 (Dlx1)
	19.2	Synaptosomal-associated protein, 25 kDa
	18.6	Protocadherin α4 (Pcdha4)
	14.1	Vesicular inhibitory amino acid transporter
	13.4	Neuron-specific gene family member 2 (Nsg2)
	11.9	Glutamic acid decarboxylase 1 (Gad1)
	10.9	Protein tyrosine phosphatase, receptor type, O
	9.46	Kinesin 2, 60/70 kDa (Kns2)
	9.19	Stathmin-like 3 (Stmn3)
	8.88	CBFA2T1-identified gene homolog
	8.71	Tubulin, β3 (Tubb3)
	8.54	Neuron-specific gene family member 1 (Nsg1)
	7.96	Ganglioside differentiation-associated protein 1
	7.54	Distalless homeobox 5 (D1x5)
	7.48	Growth-associated protein 43 (Gap43)
	6.69	Distalless homeobox 2 (D1x2)
	6.55	Doublecortin (Dcx)
	6.29	Serpini 1
	6.27	Stathmin-like 2 (Stmn2)
	6.17	α-internexin
	4.93	Synaptosomal-associated protein (Snap), 91 kDa
	4.48	Preproenkephalin 1 (Penk1)
	4.45	Neural cell adhesion molecule 1 (Ncam1)
	4.39	Stathmin 1 (Stmn1)
	4.29	Purkinje cell protein 4
	4.27	Myelin transcription factor 1-like (Myt11)
	3.70	Brain abundant signal protein 1 (Basp1)
	3.28	Tubulin, β5 (Tubb5)
	3.27	Profilin 2 (Pfn2)
	3.01	Ca-dependent activator protein for secretion
Astrocyte markers		
	16.5	Aquaporin 4 (Aqp4)
	16.3	Apolipoprotein E (Apoe)
	15.7	Paraoxonase 2 (Pon2)
	15.5	Phosphoprotein enriched in astrocytes 15
	15.5	Clusterin (Clu)
	11.2	Calizzarin (S100a11)
	8.89	Calcyclin (S100a6)
	7.54	Aldolase 3, C isoform (Aldo3)
	7.53	Peripheral myelin protein, 22 kDa (Pmp2)
	7.33	Histocompatibility 2, K region (H2-K)
	6.54	Connexin 43
	6.14	Insulin-like growth factor binding protein 5 (Igfbp5)
	6.06	Cytochrome P450, 1b1 (Cyp1b1)
	5.25	Annexin A2 (Anxa2)
	5.17	Interleukin 10 receptor, β
	4.93	*N*-Acylsphingosine amidohydrolase 1
	4.77	Histocompatibility 2, D region locus 1
	4.45	β_2-microglobulin (B2m)
	4.36	Cystatin C (Cst3)
	4.34	Nuclear factor, erythroid-derived 2-like 2
	4.09	Cd63 antigen (Cd63)
	4.00	Glutathionine-*S*-transferase, μ1 (GSTm1)
	3.96	Acid sphingomyelinase-like 3a (Asm13)
	3.59	Follistatin-like (Fst1)
	3.52	Phospholipase A2, group VII (Pla2g7)
	3.50	Lectin, galactose binding, soluble 1
	3.31	Leucine-rich repeat interacting protein 1
	3.21	Glial fibrillary acidic protein (GFAP)
	3.16	Quaking (qk)
	3.06	1-Cys peroxiredoxin (aop2)

Fold, Fold change of the vehicle-treated astrocyte-enriched cell population (GFP-positive sort) compared with the neuronal cell population (GFP-negative sort). $n = 3$ (two comparisons of sorted, 50 MOI ad-GFP-infected cultures confirmed by one comparison of sorted populations from cultures derived from GFAP-driven GFP mice).

100% of the decreased genes, in the astrocyte-enriched population. Strikingly, 100% of the increased and 79% of the decreased genes shown were completely blocked in the neuronal population. The cells in the neuronal population were not infected by ad-DN-Nrf2 (<0.1% GFP positive), suggesting that these changes are controlled through an Nrf2-dependent mechanism in the astrocytes.

A list of the genetic changes induced by tBHQ in the astrocyte-enriched (GFP-positive) and neuronal (GFP-negative) populations are shown in supplementary Tables 2 and 3, respectively (available at www.jneurosci.org). The DN column represents the change in the expression level of a gene in response to tBHQ treatment in the presence of 50 MOI of the ad-DN-Nrf2. Genes that no longer passed the rank cutoff (N/R) in the tBHQ-treated versus vehicle-treated populations indicate the involvement of Nrf2 in the induction of the gene. It is interesting to note that, in one of the most well-defined categories of ARE-driven genes, glutathione synthesis and conjugation, the vast majority of tBHQ-induced genes were not inhibited by the addition of the DN-Nrf2 virus. This may reflect differences in RNA half-life (cells were sorted only 24 hr after treatment), Nrf2 independence, or some unknown complicating factor, such as the adenovirus used.

Genes encoding cytoskeletal changes (the majority of which were increased in the astrocyte subpopulation) or serving a redundant function to other changed genes are not shown (see supplementary material). Genes that are shown have been separated into general categories according to their most applicable function. Themes altered in common between neurons and astrocytes include effects on the following: sugar synthesis and utilization, fatty acid and cholesterol utilization, detoxification and metabolism, calcium ion binding and transport, cell adhesion and integrin signaling, and synaptic activity. Of particular note are the tBHQ-mediated alterations to sugar processing apparent in the astrocyte-enriched subpopulation. The consistent changes to genes involved in sugar metabolism (glycolysis and pentose phosphate pathways, in particular) allude to astrocytic increases in energy production or storage. In addition, the marked decreased expression of interferon (IFN)-stimulated genes apparent in both subpopulations may be attributable to the actions of secreted messengers such as the IK cytokine. Consistent with previous studies correlating GSH synthesis in astrocytes to protection of neurons, the majority of previously established ARE-driven genes (bolded) involved in glutathione synthesis, metabolism, and detoxification are changed in the astrocyte-enriched, rather than the neuronal, population.

Discussion

This study demonstrates the importance of ARE activation in astrocytes of a mixed primary culture system. Data presented herein are the first demonstrating that sulforaphane activation of the ARE prevents neuronal cell death. Sulforaphane, tBHQ, and Nrf2 overexpression via adenovirus infection all induce an ARE-mediated genetic response. This response is highly selective for astrocytes over neurons and conveys neuroprotection from oxidative insults initiated by H_2O_2 or nonexcitotoxic glutamate toxicity. These two stressors target neurons preferentially over astrocytes, whereas the genetic changes induced directly by tBHQ seem to be confined to the astrocytes. Thus, a tBHQ-induced, Nrf2-dependent, coordinated change in the gene expression of astrocytes (~15% of total) is sufficient to confer protection to the majority of cortical neurons. Finally, the combined use of cell sorting and microarray technologies allowed us to determine the cell-specific changes in gene expression that facilitate ARE-mediated protection. These findings lend support to the hypothesis that treatment of cells with ARE inducers leads to modifications of glia–neuronal interactions.

It has been well established that Nrf2 is the key transcription factor mediating ARE-driven gene expression. In addition, Nrf2 knock-out cultures of primary astrocytes (Lee et al., 2003a) and neurons (Lee et al., 2003b) have been shown to be more sensitive to oxidative stressors. The complete loss of Nrf2 from mixed neural cultures, using Nrf2 knock-out mice, results in a total loss of both ARE inducibility by tBHQ and tBHQ-mediated protection from toxins (Fig. 4). Reexpression of Nrf2 using a replication-deficient adenovirus dramatically increases ARE activation and neuroprotection (Fig. 5). We also recently published that a very small percentage of ad-Nrf2-infected astrocytes (~1%) are sufficient to confer protection against oxidative glutamate toxicity toward naive cortical neurons (Shih et al., 2003). In an attempt to understand the difference between Nrf2 overexpression and ARE activation by tBHQ in this mixed culture system, we exploited the selective adenoviral infection of astrocytes to test whether tBHQ-mediated protection could be reversed by overexpression of DN-Nrf2 selectively in astrocytes. The neuroprotective effects of tBHQ were nullified, suggesting that activation of the Nrf2–ARE pathway in astrocytes alone was sufficient to confer neuroprotection. The question still remained, however, as to which genetic changes specific to astrocytes and/or neurons precipitated this protective effect.

The combined use of cell sorting and gene chip technology has allowed us to begin to determine the cell-specific contributions to ARE-mediated protection by tBHQ. Not surprisingly, the majority of the genes increased by tBHQ treatment, particularly those previously shown to be ARE-driven, were seen in the astrocyte-enriched population. There were, however, many genes that changed in both the neuronal and astrocyte-enriched populations, indicating either stimulation of the ARE in both or induced changes in one population by the other. Genes increased in concert include GSTm1, malic enzyme, stearoyl-CoA desaturases (Scd), and glucose phosphate isomerase (GPI). More striking were the genes decreased in both of the sorted populations. These include Notch 1, cyclin D2, p21, MAP tau, and thymopoietin, most of which regulate cell cycle events. In addition, there were dramatic tBHQ-induced changes to protein modification, calcium homeostasis, and intracellular phosphorylation cascades [including TGFβ, insulin, and nuclear factor-κB (NF-κB) pathways]. These alterations may modify multiple facets of the complex signaling systems directing cellular events.

The most intriguing aspect of observing ARE activity in a mixed culture system is the presence of communication between astrocytes and neurons. Astrocyte–neuron interactions are proposed to be involved in synapse formation and conduction, neurotransmitter release, process outgrowth, chemotaxis, energy production, and response to injury (Pellerin and Magistretti, 1994; Dugan et al., 1995; Vernadakis, 1996; Pellerin et al., 1998; Goritz et al., 2002). The modified genetic profile of ARE-activated astrocytes alludes to an enhancement of environmental detoxification and increased trophic factor secretion.

Most noticeable of the changes induced by tBHQ specifically in the astrocyte-enriched population is the large increase in cellular protective proteins. A battery of ARE-driven genes encoding detoxification enzymes were upregulated, as were enzymes associated with glutathione synthesis and conjugation reactions, although the latter were not significantly inhibited by DN-Nrf2 (supplementary Table 2, available at www.jneurosci.org). Interestingly, in addition to regulating the neural environment, astro-

cytes help to synthesize neuronal glutathione (Aschner, 2000). Thus, the astrocyte-dependent environmental detoxification that contributes to neuronal protection is, at least in part, regulated by this inducible system.

A striking number of genes associated with energy production were upregulated by tBHQ in the glia-enriched population, including the majority of the 10 genes catalyzing the glycolysis of glucose to pyruvate. Glucose metabolism is essential for calcium homeostasis in the brain via the synthesis of ATP (Nijjar and Belgrave, 1997). In addition, pyruvate can be further metabolized to lactate, the preferred energy substrate for neurons that helps to maintain synaptic transmission (Pellerin and Magistretti, 1994; Pellerin et al., 1998). The increases in astrocytic glycogen synthesis (glucan branching enzyme), gluconeogenesis (GPI), and neuronal creatine production [Gatm (glycine amidinotransferase) and creatine kinase] may also indicate an enhanced maintenance of neuronal activity by tBHQ. Interestingly, astrocytes are known to couple neuronal activity (glutamate release) to energy production and glutathione synthesis (Magistretti et al., 1999; Sonnewald et al., 2002). Additional metabolism of pyruvate to acetyl CoA leads to an increased synthesis of cholesterol (squalene epoxidase and lanosterol synthase) and fatty acids for phospholipids and energy storage (malic enzyme, fatty acid synthase, and Scd1 and -2). Increasingly, research reveals that neurons require glia-derived cholesterol to form efficient synaptic connections (Barres and Smith, 2001; Goritz et al., 2002; Pfrieger, 2003). Thus, stimulated astrocytes may, in addition to detoxification of the cellular environment, produce increasing levels of substrates essential for neuronal maintenance. An enhanced coupling of metabolism and energy utilization between astrocytes and neurons appears to be a key mechanism underlying tBHQ-inducible neuroprotection.

In addition to metabolic changes, cells responding to tBHQ treatment are modified in their extracellular interactions. An enhancement of physical interactions would help to facilitate much of the soluble and contact-dependent communication between neurons and glia. In the astrocyte-enriched subpopulation, tBHQ increased integrin signaling molecules [calpain, Nap1 (NCK-associated protein 1), and Thy1 (thymus cell antigen 1)], as well as cell adhesion proteins (fibronectin and laminin). These factors and integrin receptors are partially responsible for initiating neuron–glia interactions (Marchetti, 1997; Bialkowska et al., 2000; Leyton et al., 2001; Ding et al., 2002). In neurons, the elevated expression of neuropilin, calmyrin, and VCAM (vascular cell adhesion molecule) supports a tBHQ-induced enhancement of cellular contacts.

Astrocytes play a considerable role in neuronal synapse formation (Goritz et al., 2002; Pfrieger, 2003). In addition to glia-derived cholesterol and lactate, neurons are thought to require astrocytes during synapse maturation for soluble and contact-dependent factors. GABAergic signaling has been implicated in ARE activity (supplementary Table 3, available at www.jneurosci.org) (Lee et al., 2003b) and has been postulated to mediate neuron-to-glia signaling (Runquist and Alonso, 2003). Astrocytes respond to, and secrete, such neurochemicals (Danbolt, 2001; Fields and Stevens-Graham, 2002). Some genes increased in the astrocyte-enriched population are Rapsyn, neuroserpin, and syntaxin bp (binding protein) 3. Rapsyn clusters acetylcholine receptors; neuroserpin protects against plasminogen activators and helps form synapses; and syntaxin bp3 contributes to synaptic trafficking and glucose transport. In the neuronal subpopulation, transcripts for FGF14, a factor essential for synaptosomal function (Wang et al., 2002), synaptotagmins, which are essential for calcium-dependent synaptic vesicle docking, and galanin, which maintains neurotransmitter homeostasis, are all increased by tBHQ. Thus, it appears that tBHQ-induced astrocytes may be better primed to receive signals from neighboring neurons inducing motility, adhesion, or morphogenesis to facilitate energy and cholesterol production necessary for synapse formation and maintenance.

The ARE-inducible transmembrane and secreted proteins from both populations may be the direct mediators of astrocytic protection of neurons against insult. Basigin, a transmembrane glycoprotein, has been shown to induce the regrowth of damaged dopaminergic fibers after exposure to 1-methyl-4-phenylpyridinium (Mitsumoto et al., 2001). Gdf15 (growth/differentiation factor-15) is a secreted TGFβ family member that acts as a direct trophic factor for neurons (Strelau et al., 2000). CREG (cellular repressor of E1A genes) is a secreted glycoprotein that antagonizes E1A, an inhibitor of Nrf2 activity (Katoh et al., 2001). Endothelin-1 has been shown to increase astrocytic glial-derived neurotrophic factor secretion, induce extracellular and cytoskeletal reorganization, and protect against hypoxia and ischemia (Ho et al., 2001; Egnaczyk et al., 2003). Interestingly, the IK cytokine prevents immune response by inhibiting IFN-γ-induced [human leukocyte antigen (HLA) class II] gene expression (Krief et al., 1994). Transcripts induced by IFN were significantly decreased in both populations, whereas an HLA repressor, NFX1, was increased. This suggests a link between increased IK mRNA and resultant changes to gene expression. These factors, in conjunction with Thy1, FGF14, lactate, cholesterol, and glutathione, may comprise the soluble mediators of neuron–glia communication effecting neuroprotection.

The progressive neurodegeneration seen in many diseases of aging is due, in part, to the buildup of harmful oxidants. As a result of this toxin accumulation, these neurons display decreased synaptic efficiency or undergo cell death. Selective chemical activation of the ARE in astrocytes may provide a means of amplifying the existing metabolic, soluble, and physical coupling between astrocytes and neurons to boost synaptic function and provide protection against oxidative injury. Future work will confirm and analyze these changes within the intact architecture of the brain to pinpoint the exact protective mechanism(s) underlying this enhanced interaction *in vivo*.

References

Ahlgren-Beckendorf JA, Reising AM, Schander MA, Herdler JW, Johnson JA (1999) Coordinate regulation of NAD(P)H:quinone oxidoreductase and glutathione-*S*-transferases in primary cultures of rat neurons and glia: role of the antioxidant/electrophile responsive element. Glia 25:131–142.

Alam J, Stewart D, Touchard C, Boinapally S, Choi AM, Cook JL (1999) Nrf2, a Cap'n'Collar transcription factor, regulates induction of the heme oxygenase-1 gene. J Biol Chem 274:26071–26078.

Aschner M (2000) Neuron-astrocyte interactions: implications for cellular energetics and antioxidant levels. Neurotoxicology 21:1101–1107.

Barres BA, Smith SJ (2001) Neurobiology. Cholesterol-making or breaking the synapse. Science 294:1296–1297.

Bialkowska K, Kulkarni S, Du X, Goll DE, Saido TC, Fox JE (2000) Evidence that β_3 integrin-induced Rac activation involves the calpain-dependent formation of integrin clusters that are distinct from the focal complexes and focal adhesions that form as Rac and RhoA become active. J Cell Biol 151:685–696.

Chan K, Lu R, Chang JC, Kan YW (1996) NRF2, a member of the NFE2 family of transcription factors, is not essential for murine erythropoiesis, growth, and development. Proc Natl Acad Sci USA 93:13943–13948.

Chanas SA, Jiang Q, McMahon M, McWalter GK, McLellan LI, Elcombe CR, Henderson CJ, Wolf CR, Moffat GJ, Itoh K, Yamamoto M, Hayes JD (2002) Loss of Nrf2 transcription factor causes a marked reduction in constitutive and inducible expression of the glutathione *S*-transferase *Gsta1*, *Gsta2*, *Gstm1*, *Gstm2*, *Gstm3*, *Gstm4* genes in the livers of male and female mice. Biochem J 365:405–416.

Coyle JT, Puttfarcken P (1993) Oxidative stress, glutamate, and neurodegenerative disorders. Science 262:689–695.

Danbolt NC (2001) Glutamate uptake. Prog Neurobiol 65:1–105.

Ding Q, Stewart Jr J, Prince CW, Chang PL, Trikha M, Han X, Grammer JR, Gladson CL (2002) Promotion of malignant astrocytoma cell migration by osteopontin expressed in the normal brain: differences in integrin signaling during cell adhesion to osteopontin versus vitronectin. Cancer Res 62:5336–5343.

Dinkova-Kostova AT, Holtzclaw WD, Cole RN, Itoh K, Wakabayashi N, Katoh Y, Yamamoto M, Talalay P (2002) Direct evidence that sulfhydryl groups of Keap1 are the sensors regulating induction of phase 2 enzymes that protect against carcinogens and oxidants. Proc Natl Acad Sci USA 99:11908–11913.

Duffy S, So A, Murphy TH (1998) Activation of endogenous antioxidant defenses in neuronal cells prevents free radical-mediated damage. J Neurochem 71:69–77.

Dugan LL, Bruno VM, Amagasu SM, Giffard RG (1995) Glia modulate the response of murine cortical neurons to excitotoxicity: glia exacerbate AMPA neurotoxicity. J Neurosci 15:4545–4555.

Eftekharpour E, Holmgren A, Juurlink BH (2000) Thioredoxin reductase and glutathione synthesis is upregulated by *t*-butylhydroquinone in cortical astrocytes but not in cortical neurons. Glia 31:241–248.

Egnaczyk GF, Pomonis JD, Schmidt JA, Rogers SD, Peters C, Ghilardi JR, Mantyh PW, Maggio JE (2003) Proteomic analysis of the reactive phenotype of astrocytes following endothelin-1 exposure. Proteomics 3:689–698.

Fernandez-Checa JC, Kaplowitz N, Garcia-Ruiz C, Colell A, Miranda M, Mari M, Ardite E, Morales A (1997) GSH transport in mitochondria: defense against TNF-induced oxidative stress and alcohol-induced defect. Am J Physiol 273:G7–G17.

Fields RD, Stevens-Graham B (2002) New insights into neuron-glia communication. Science 298:556–562.

Goritz C, Mauch DH, Nagler K, Pfrieger FW (2002) Role of glia-derived cholesterol in synaptogenesis: new revelations in the synapse-glia affair. J Physiol (Paris) 96:257–263.

Hardy S, Kitamura M, Harris-Stansil T, Dai Y, Phipps ML (1997) Construction of adenovirus vectors through Cre-lox recombination. J Virol 71:1842–1849.

Hertz L, Juurlink B, Szuchet S, Walz W (1985) Cell and tissue cultures. Neuromethods 1:117–167.

Ho MC, Lo AC, Kurihara H, Yu AC, Chung SS, Chung SK (2001) Endothelin-1 protects astrocytes from hypoxic/ischemic injury. FASEB J 15:618–626.

Johnson DA, Andrews GK, Xu W, Johnson JA (2002) Activation of the antioxidant response element in primary cortical neuronal cultures derived from transgenic reporter mice. J Neurochem 81:1233–1241.

Kang KW, Lee SJ, Park JW, Kim SG (2002) Phosphatidylinositol 3-kinase regulates nuclear translocation of NF-E2-related factor 2 through actin rearrangement in response to oxidative stress. Mol Pharmacol 62:1001–1010.

Katoh Y, Itoh K, Yoshida E, Miyagishi M, Fukamizu A, Yamamoto M (2001) Two domains of Nrf2 cooperatively bind CBP, a CREB binding protein, and synergistically activate transcription. Genes Cells 6:857–868.

Krief P, Augery-Bourget Y, Plaisance S, Merck MF, Assier E, Tanchou V, Billard M, Boucheix C, Jasmin C, Azzarone B (1994) A new cytokine (IK) down-regulating HLA class II: monoclonal antibodies, cloning and chromosome localization. Oncogene 9:3449–3456.

Lee JM, Hanson JM, Chu WA, Johnson JA (2001) Phosphatidylinositol 3-kinase, not extracellular signal-regulated kinase, regulates activation of the antioxidant-responsive element in IMR-32 human neuroblastoma cells. J Biol Chem 276:20011–20016.

Lee JM, Calkins MJ, Chan K, Kan YW, Johnson JA (2003a) Identification of the NF-E2-related factor-2-dependent genes conferring protection against oxidative stress in primary cortical astrocytes using oligonucleotide microarray analysis. J Biol Chem 278:12029–12038.

Lee JM, Shih AY, Murphy TH, Johnson JA (2003b) NF-E2-related factor 2 mediates neuroprotection against mitochondrial complex I inhibitors and increased concentrations of intracellular calcium in primary cortical neurons. J Biol Chem 278:37948–37956.

Leyton L, Schneider P, Labra CV, Ruegg C, Hetz CA, Quest AF, Bron C (2001) Thy-1 binds to integrin β_3 on astrocytes and triggers formation of focal contact sites. Curr Biol 11:1028–1038.

Li J, Johnson JA (2002) Time-dependent changes in ARE-driven gene expression by use of a noise-filtering process for microarray data. Physiol Genomics 9:137–144.

Li P, Nijhawan D, Budihardjo I, Srinivasula SM, Ahmad M, Alnemri ES, Wang X (1997) Cytochrome *c* and dATP-dependent formation of Apaf-1/caspase-9 complex initiates an apoptotic protease cascade. Cell 91:479–489.

Li J, Lee JM, Johnson JA (2002) Microarray analysis reveals an antioxidant responsive element-driven gene set involved in conferring protection from an oxidative stress-induced apoptosis in IMR-32 cells. J Biol Chem 277:388–394.

Magistretti PJ, Pellerin L, Rothman DL, Shulman RG (1999) Energy on demand. Science 283:496–497.

Marchetti B (1997) Cross-talk signals in the CNS: role of neurotrophic and hormonal factors, adhesion molecules and intercellular signaling agents in luteinizing hormone-releasing hormone (LHRH)-astroglial interactive network. Front Biosci 2:d88–d125.

Marini MG, Chan K, Casula L, Kan YW, Cao A, Moi P (1997) hMAF, a small human transcription factor that heterodimerizes specifically with Nrf1 and Nrf2. J Biol Chem 272:16490–16497.

Mattson MP (2000) Apoptosis in neurodegenerative disorders. Nat Rev Mol Cell Biol 1:120–129.

Mitsumoto Y, Watanabe A, Miyauchi T, Jimma F, Moriizumi T (2001) Stimulation of the regrowth of MPP^+-damaged dopaminergic fibers by the treatment of mesencephalic cultures with basigin. J Neural Transm 108:1127–1134.

Moehlenkamp JD, Johnson JA (1999) Activation of antioxidant/electrophile-responsive elements in IMR-32 human neuroblastoma cells. Arch Biochem Biophys 363:98–106.

Moi P, Chan K, Asunis I, Cao A, Kan YW (1994) Isolation of NF-E2-related factor 2 (Nrf2), a NF-E2-like basic leucine zipper transcriptional activator that binds to the tandem NF-E2/AP1 repeat of the β-globin locus control region. Proc Natl Acad Sci USA 91:9926–9930.

Murphy TH, Miyamoto M, Sastre A, Schnaar RL, Coyle JT (1989) Glutamate toxicity in a neuronal cell line involves inhibition of cystine transport leading to oxidative stress. Neuron 2:1547–1558.

Murphy TH, Schnaar RL, Coyle JT (1990) Immature cortical neurons are uniquely sensitive to glutamate toxicity by inhibition of cystine uptake. FASEB J 4:1624–1633.

Murphy TH, De Long MJ, Coyle JT (1991) Enhanced NAD(P)H:quinone reductase activity prevents glutamate toxicity produced by oxidative stress. J Neurochem 56:990–995.

Murphy TH, Yu J, Ng R, Johnson DA, Shen H, Honey CR, Johnson JA (2001) Preferential expression of antioxidant response element mediated gene expression in astrocytes. J Neurochem 76:1670–1678.

Nguyen T, Huang HC, Pickett CB (2000) Transcriptional regulation of the antioxidant response element. Activation by Nrf2 and repression by MafK. J Biol Chem 275:15466–15473.

Nijjar M, Belgrave RL (1997) Regulation of Ca^{2+} homeostasis by glucose metabolism in rat brain. Mol Cell Biochem 176:317–326.

Pellerin L, Magistretti PJ (1994) Glutamate uptake into astrocytes stimulates aerobic glycolysis: a mechanism coupling neuronal activity to glucose utilization. Proc Natl Acad Sci USA 91:10625–10629.

Pellerin L, Pellegri G, Bittar PG, Charnay Y, Bouras C, Martin JL, Stella N, Magistretti PJ (1998) Evidence supporting the existence of an activity-dependent astrocyte-neuron lactate shuttle. Dev Neurosci 20:291–299.

Pfrieger FW (2003) Role of cholesterol in synapse formation and function. Biochim Biophys Acta 1610:271–280.

Ramos-Gomez M, Kwak MK, Dolan PM, Itoh K, Yamamoto M, Talalay P, Kensler TW (2001) Sensitivity to carcinogenesis is increased and chemoprotective efficacy of enzyme inducers is lost in nrf2 transcription factor-deficient mice. Proc Natl Acad Sci USA 98:3410–3415.

Runquist M, Alonso G (2003) GABAergic signaling mediates the morphological organization of astrocytes in the adult rat forebrain. Glia 41:137–151.

Rushmore TH, Kong AN (2002) Pharmacogenomics, regulation and signaling pathways of phase I and II drug metabolizing enzymes. Curr Drug Metab 3:481–490.

Rushmore TH, King RG, Paulson KE, Pickett CB (1990) Regulation of glutathione *S*-transferase Ya subunit gene expression: identification of a unique xenobiotic-responsive element controlling inducible expression by planar aromatic compounds. Proc Natl Acad Sci USA 87:3826–3830.

Rushmore TH, Morton MR, Pickett CB (1991) The antioxidant responsive element. Activation by oxidative stress and identification of the DNA consensus sequence required for functional activity. J Biol Chem 266:11632–11639.

Shih AY, Johnson DA, Wong G, Kraft AD, Jiang L, Erb H, Johnson JA, Murphy TH (2003) Coordinate regulation of glutathione biosynthesis and release by Nrf2-expressing glia potently protects neurons from oxidative stress. J Neurosci 23:3394–3406.

Simonian NA, Coyle JT (1996) Oxidative stress in neurodegenerative diseases. Annu Rev Pharmacol Toxicol 36:83–106.

Sonnewald U, Qu H, Aschner M (2002) Pharmacology and toxicology of astrocyte-neuron glutamate transport and cycling. J Pharmacol Exp Ther 301:1–6.

Strelau J, Sullivan A, Bottner M, Lingor P, Falkenstein E, Suter-Crazzolara C, Galter D, Jaszai J, Krieglstein K, Unsicker K (2000) Growth/differentiation factor-15/macrophage inhibitory cytokine-1 is a novel trophic factor for midbrain dopaminergic neurons in vivo. J Neurosci 20: 8597–8603.

Tietze F (1969) Enzymic method for quantitative determination of nanogram amounts of total and oxidized glutathione: applications to mammalian blood and other tissues. Anal Biochem 27:502–522.

Vernadakis A (1996) Glia-neuron intercommunications and synaptic plasticity. Prog Neurobiol 49:185–214.

Wang Q, Bardgett ME, Wong M, Wozniak DF, Lou J, McNeil BD, Chen C, Nardi A, Reid DC, Yamada K, Ornitz DM (2002) Ataxia and paroxysmal dyskinesia in mice lacking axonally transported FGF14. Neuron 35:25–38.

Zhuo L, Sun B, Zhang CL, Fine A, Chiu SY, Messing A (1997) Live astrocytes visualized by green fluorescent protein in transgenic mice. Dev Biol 187: 36–42.